JOURNAL OF AIRCRAFT
Vol. 37, No. 4, July–August 2000

Implications of Recent Rotary Rig Results for Flight Prediction

Martin E. Beyers*
Institute for Aerospace Research/NRC, Ottawa, Ontario K1A 0R6, Canada
and
Lars E. Ericsson†
Mountain View, California 94040

Analysis of rotary balance data on a generic aircraft model revealed the nature of the flow mechanisms present in subscale experiments, which included the existence of support interference. Recent results on the F/A-l8 confirmed the existence of a threshold rotation rate in the rotary data and revealed that in the nonlinear domain at elevated angles of attack, alternatively deterministic or chaotic behavior will prevail, depending on whether or not the magnitude of the initial rotation rate exceeds the threshold value. This has important implications for flight mechanics predictions and control system design as the poststall maneuvering envelope often will include the hysteresis loop. Moreover, dynamic data generated to date in the nonlinear domain have often been restricted to this inner region, limited by the threshold rates, and do not provide any information about the basic hysteretic behavior. Only a comprehensive investigation of steady-state hysteresis and support interference, as in the case of the F/A-18, can provide the basis needed for flight predictions in this domain.

Nomenclature

b = wing span
d = maximum body diameter
l = rolling moment: coefficient $C_l = l/(\rho_\infty U_\infty^2/2)Sb$
n = yawing moment: coefficient $C_n = n/(\rho_\infty U_\infty^2/2)Sb$
Re = Reynolds number based on d and freestream conditions
S = reference area (projected wing area)
t = time
U_∞ = freestream velocity
$\bar{U}$ = mean convection velocity
α = angle of attack
θ_A = forebody apex half-angle
ρ = air density
Φ_m = azimuth angle
Ω = dimensionless coning rate, $\omega b/2U_\infty$
ω = coning rate

Subscripts

on = onset of asymmetry
S = sting
s = start
T = threshold
∞ = freestream conditions

Superscript

$(\dot{\ })$ = differentiation with respect to time

Introduction

THE prediction of full-scale maneuvering flight using subscale wind-tunnel data is a concern to the aircraft designer. The immediate challenge, before the extrapolation to full scale[1] can be contemplated, is the determination of the free-flight characteristics at the model scale,[2] where scale-dependent fluid/motion coupling[3,4] and ground-test facility interference effects[5,6] are present. As a result of these flowfield interactions, the aerodynamics of the model are generally more complex than that of the aircraft in free flight. Flight mechanics predictions in the poststall domain rely heavily on the experimental dynamic database.[7] This is particularly true in the case of rotary balance data, which provide the aerodynamic reactions to the most basic nonplanar characteristic motion, namely, coning, needed to simulate high-alpha maneuvers. The rotary aerodynamics are highly nonlinear, and it is necessary to define the steady-state hysteresis when it is present.

In Ref. 2 the present authors investigated the nature of the flow mechanisms present in subscale experiments of the AGARD WG16A model[8] (Fig. 1) and linked the effects of these mechanisms to the existence of different flow states. The existence of a threshold rotation rate Ω_T, which signals the unsteadiness preceding bifurcation in the rotary data, was postulated.[2] Although the greater complexity of the aerodynamic responses in the subscale tests was revealed, it was evident that the data were too sparse to permit conclusive interpretation.[2] This raised the question as to whether the steady-state hysteresis behavior had been adequately determined in the AGARD tests. In more recent experiments on the F/A-18 (Fig. 2)[9,10] definitive steady-state hysteresis characteristics were identified in the range of asymmetric vortex shedding.[11] The results yielded evidence of several unsteady flow mechanisms and demonstrated the importance of time-history effects for the case of sustained rotational motion.

Separated Flow/Motion Coupling Mechanisms

The principal flow mechanisms determining the lateral-directional aerodynamics of a configuration having a slender forebody with wing leading-edge extensions (LEXs) are the moving wall effect[4] and the coning-induced LEX upwash effect.[12] Figures 3a–3c illustrate the crossflow conditions on a coning slender forebody in laminar, turbulent, and critical crossflow, respectively.[4] In the subcritical and supercritical cases the moving wall effects[4] on the boundary layer in the stagnation region will cause flow separation to be delayed on the advancing side and promoted on the receding side, which generates a prospin force, as has been demonstrated.[3,4] As a result of this flow separation asymmetry, the vortex on the advancing side remains attached whereas on the retreating side it lifts off, as in the case of a cone–cylinder[13] coning at $Re \cong 10^5$ (Fig. 4). At transitional flow conditions the crossflow asymmetry is reversed[4] through the fluid/motion coupling effect on flow separation that occurs through the moving wall effect on boundary-layer transition[14] (Fig. 3c). Kinematic coupling may also be present.[7] It has been found that when the LEX surfaces start at the base of the slender forebody,

Received 18 October 1999; revision received 21 February 2000; accepted for publication 25 February 2000.

*Head Aircraft Aerodynamics Group, Aerodynamics Laboratory. Senior Member AIAA.
†Consulting Engineer. Fellow AIAA.

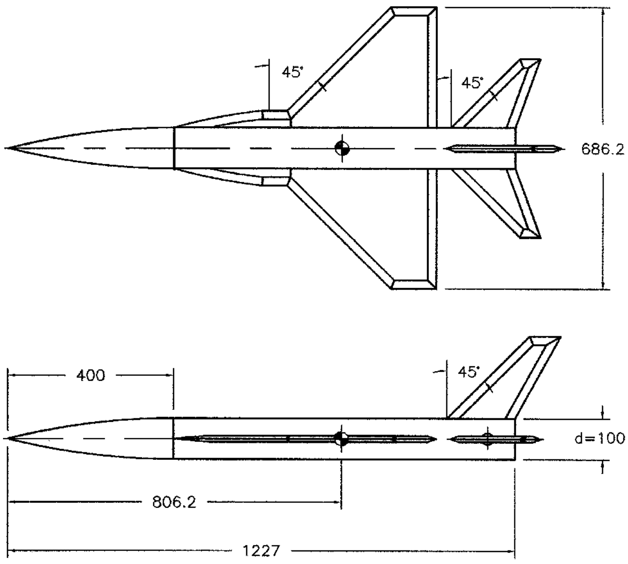

Fig. 1 AGARD model WG16A.

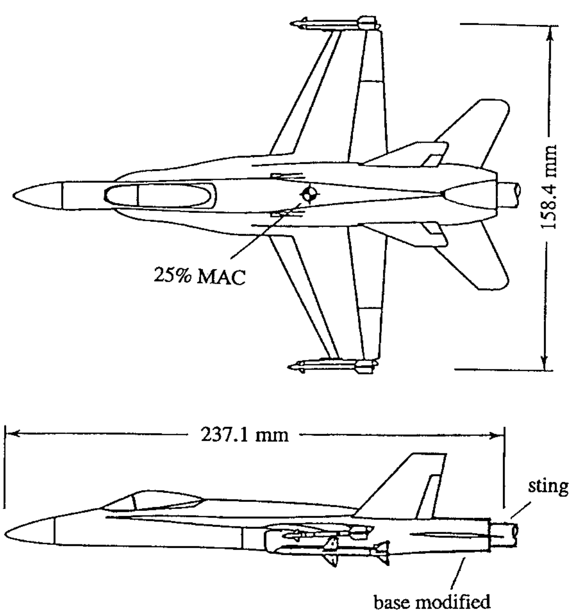

Fig. 2 Model of 1/72-scale F/A-18.

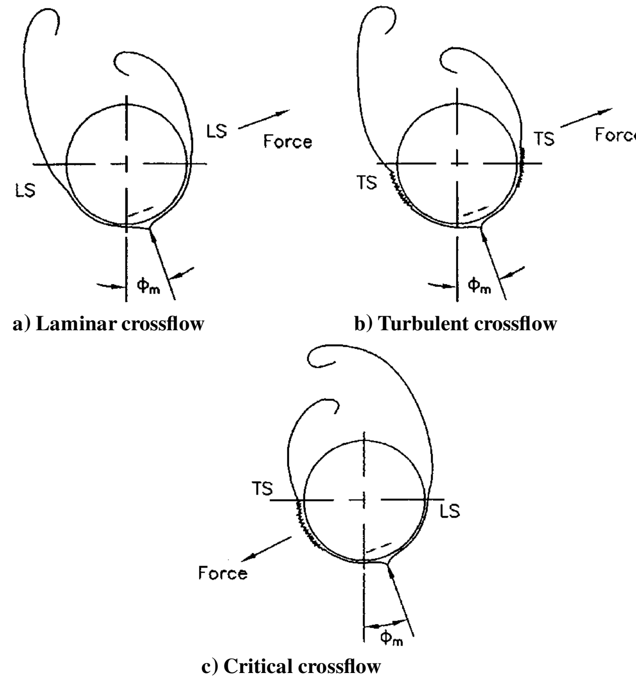

Fig. 3 Crossflow separation characteristics for translating circular cross section.

the coning-induced LEX upwash on the forebody in the presence of local sideslip tends to overpower the viscous moving wall effect.[12] This effect of the LEX-induced upwash on the crossflow separation asymmetry is illustrated in Fig. 5. The coning motion generates a sideslip distribution that decreases the effective leading-edge sweep on the advancing side and increases it on the receding side. The result is increased/decreased LEX-induced upwash on the advancing/receding sides, respectively, generating the crossflow separation characteristics sketched in Fig. 5b. Vortex liftoff takes place on the advancing side, as demonstrated by water-tunnel results for the coning WG16A model[8] (Fig. 6). This situation prevails while the angle of attack increases, but the effect diminishes as the vortex-induced lift on the LEX is decreased by advancing vortex breakdown. When vortex breakdown reaches the LEX apex, the so-called three-dimensional stall[15] occurs, with the flow separation extending along the full length of the windward leading edge of the LEX, which creates a region of low energy flow. In the case of coning motion the obstruction caused by the shear layer enclosing this large separation bubble precipitates the early separation of the windward boundary layer on the forebody, thereby maintaining the crossflow separation asymmetry of the type illustrated in Fig. 5b to high angles of attack.

When in rotary testing the coning rate is increased from $\Omega = 0$, the flowfield inertia tends to keep the flow separation asymmetry locked in to the configuration initially set by the combined effects of forebody microasymmetry[16] and flow asymmetry due to support interference.[5] The various flow mechanisms generated by the coning motion will combine to reinforce the initial flow asymmetry, or oppose it. These are competing flow mechanisms, but in the presence of sustained motion a single flow mechanism is likely to dominate and either reinforce or oppose the initial flow separation asymmetry. Because there is a great resistance to change in the flowfield once the asymmetry is locked in at $\alpha > \alpha_{\mathrm{on}}$, a dominant flow mechanism will be required to alter the flow state. The point at which this occurs is a critical point, identified by the threshold coning rate Ω_T.

Generic Slender Forebody/LEX Configuration

Although the AGARD WG16A model (Fig. 1) has been tested with and without forebody strakes and boundary-layer trips, only the data obtained with the clean forebody will be used. All of the forebody flow mechanisms just described are thought to play a role at $\alpha \geq 30$ deg ($2\theta_A = 28.5$ deg), resulting in the observed highly complex aerodynamic responses.[2] As already noted, when lateral motion is present, one mechanism generally will dominate. However, interference from the rotary rig[5] (Fig. 7), as well as the moving wall effect,[4] are likely to have played significant roles at $\alpha > 2\theta_A$, which adds to the unsteadiness and leads to multiple flow states. This was recognized in Ref. 2, and a possible explanation for the observed complex behavior was postulated. There was, however, insufficient data available to define the multiple flow states. For one thing, the steady-state hysteresis had not been determined. Moreover, as rotary balance measurements represent time-averaged values over a number of complete rotations, they do not offer the explicit information about the unsteadiness needed to provide a complete interpretation of the prevailing fluid mechanical processes.

The experimental results for body-alone (Fig. 8) show that for $\alpha = 40$, 50, and 60 deg, a significant negative yawing moment was measured for $\Omega = 0$, caused by nose microasymmetry.[16] For a positive coning rate, $\Omega > 0$, the critical moving wall effect (Fig. 3c) will generate a negative C_n contribution, producing the measured damping trend in Fig. 8. Correspondingly, a negative coning rate,

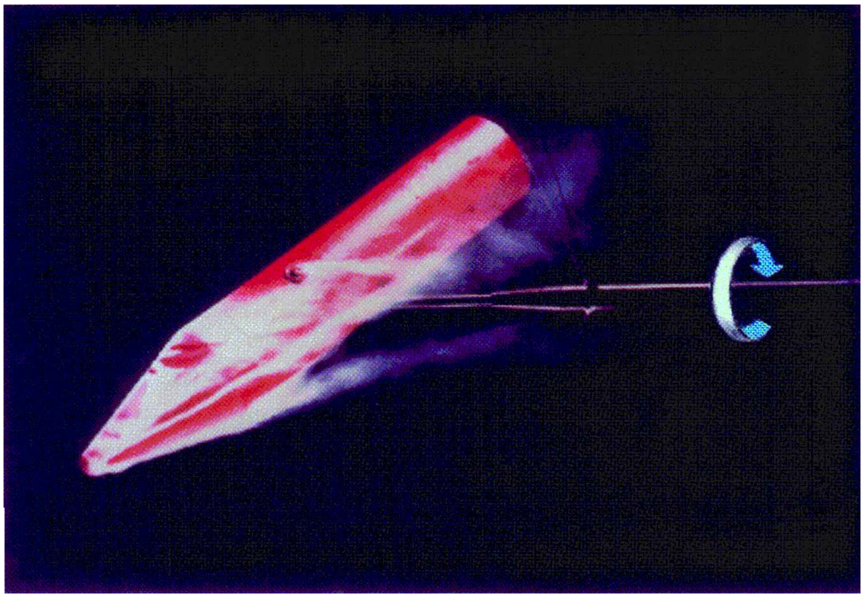

Fig. 4 Flow visualization of 15-deg cone–cylinder model coning at subcritical Reynolds number (clockwise rotation).[13]

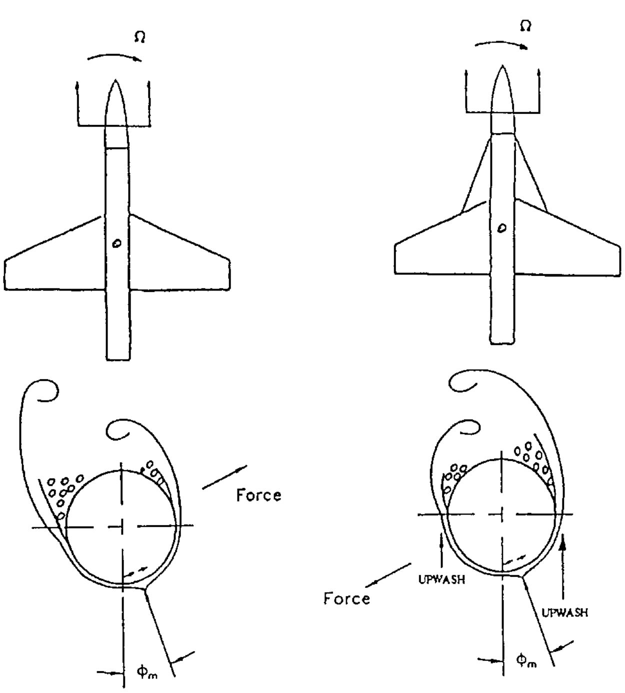

a) Without LEXs **b) With LEXs**

Fig. 5 Conceptual crossflow separation on the slender forebody of a coning aircraft model.

$\Omega < 0$, will produce damping by generating a positive C_n contribution. This $C_n(\Omega)$ trend is observed for $\alpha = 30$ and 40 deg, but not for $\alpha = 50$ deg, where the $C_n(\Omega)$ slope approaches zero for $\Omega < 0$ before a discontinuous change to a positive C_n occurs at $-0.06 < \Omega < -0.05$. At $\Omega \leq -0.06$ the $C_n(\Omega)$ characteristics exhibit a damping slope that is roughly the same as for $\Omega \geq 0.06$. Looking at the corresponding $C_n(\Omega)$ slopes for $\alpha = 40$ deg, it appears that a discontinuous change to positive C_n values would have occurred if the test range had been extended beyond $\Omega = -0.16$. The effect of the support on the discontinuous change of $C_n(\Omega)$ is the expected result of the interaction of the vortical wake from the nose with the downstream rotary rig support (Fig. 7). Similar results were obtained at $\alpha = 70$ deg with an F-15 model with nose boom, using a dorsal sting support from the C strut[5,17] (Fig. 9). Figure 9 shows that at $Re = 1.5 \times 10^6$, the $C_n(\Omega)$ discontinuities were generated by the vortex wake interacting with the dorsal sting support inclined at $\alpha_S = 70$ deg, rather than with the downstream C strut (Fig. 7), as in the present case. The results show a high sensitivity to Reynolds number even for turbulent crossflow Reynolds numbers on the nose, which indicates that at $Re = 1.5 \times 10^6$, the early transitional flow region on the nose boom had created the Reynolds-number-sensitive nose microasymmetry discussed in Refs. 16 and 18. This Reynolds number sensitivity is likely to have played a role in the documented nonrepeatability of the $C_n(\Omega)$ hysteresis loops.

By the comparison of $C_n(\Omega)$ data at $\alpha = 50$ deg for body alone (Fig. 8) and for the complete clean configuration (Fig. 10) it can be seen that there is good agreement up to a point. That is, the body-alone $C_n(\Omega)$ characteristics can represent the aerodynamics of the vehicle at low Ω, albeit at different Reynolds numbers (subcritical data were not available for body-alone). The static intercept and slope at $\Omega \rightarrow 0$ agree well, but at $|\Omega| > 0.05$ the curves diverge at the point where the data scatter increases. At $\Omega < 0$ the slope is near zero in both cases as the bifurcation point is approached.

When we look at the threshold $\Omega_T = -0.05$, it is at first surprising to find it to be the same at $\alpha = 50$ deg for body-alone (Fig. 8) and the complete configuration (Fig. 10). Based on the flow picture presented in Fig. 5, one would expect them to be different. The explanation is the difference in Reynolds numbers, $Re = 0.3 \times 10^6$ in Fig. 8 compared to $Re = 0.2 \times 10^6$ in Fig. 10. For the laminar flow conditions existing at $Re = 0.2 \times 10^6$, one would expect Fig. 8 to have exhibited the forebody crossflow characteristics shown in Fig. 5a, and Ω_T could not have been the same as in Fig. 10. However, the results in Fig. 8 are for $Re = 0.3 \times 10^6$ and produce the critical crossflow characteristics illustrated in Fig. 3c and give the same type of separation asymmetry on the forebody as that produced by the LEX-induced upwash effect in Fig. 5b. The similar crossflow separation characteristics will produce similar off-surface flow structures, and the interactions with the model support will be similar. This explains the existence of a common threshold rate condition in the two cases.

The absence of significant data scatter at $|\Omega| < 0.05$ may be indicative of the high flow inertia resulting from the stabilizing effect of the flow asymmetry at $\alpha = 50$ deg $\gg 2\theta_A$, where the forebody microasymmetry effect is reinforced by the asymmetry generated by support interference. At $\Omega < 0$ the $C_n(\Omega)$ characteristics remained essentially constant until the coning-induced lateral displacement of the vortical wake was large enough to cause a reversal of the flow separation asymmetry. The difference in $C_n(\Omega)$ characteristics at $|\Omega| > 0.05$ for the complete configuration (Fig. 10) and body-alone (Fig. 8) reflects the difference in the sensitivity to the coning rate of

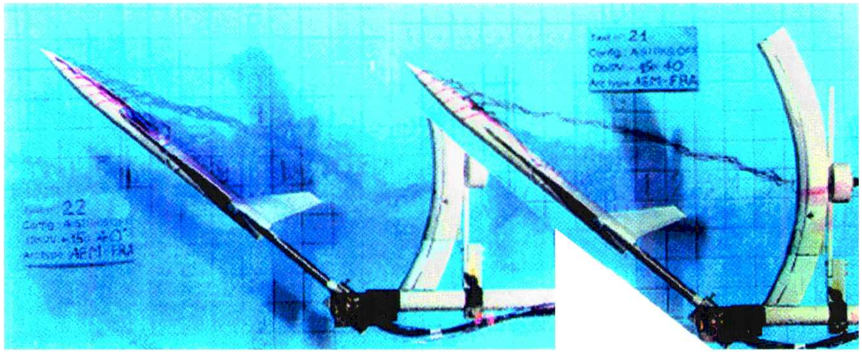

(a) Ω = 0.15 (b) Ω = −0.15

Fig. 6 Vortex flow on AGARD WG16A model coning at α = 40 deg and Ω = ± 0.15 (Ref. 8).

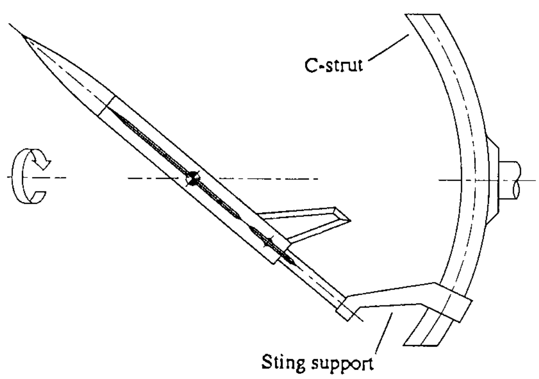

Fig. 7 Schematic of rotary rig support.

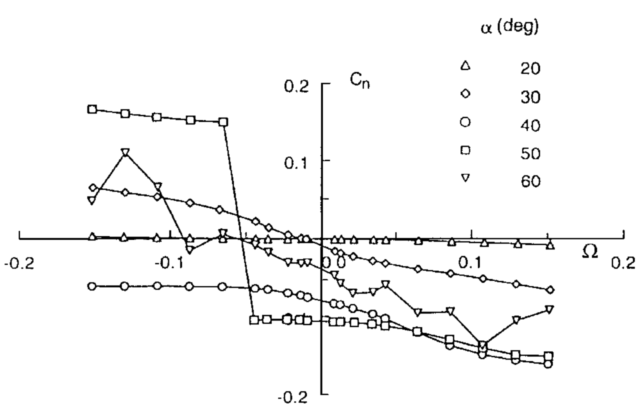

Fig. 8 Body-alone $C_n(\Omega)$ characteristics of AGARD WG16A model at $Re = 0.3 \times 10^6$ (Ref. 8).

the LEX-induced upwash effect and the critical moving wall effect in directing the vortical wake from the nose. At $|\Omega| > |\Omega_T| = 0.05$, the dominance of the LEX-induced upwash effect is lost when vortex breakdown on the windward LEX reaches the apex and only the LEX bubble effect remains. In the body-alone case the Reynolds number was critical at $Re = 0.3 \times 10^6$ and the $C_n(\Omega)$ trend continues to be damped even as the rate is increased (Fig. 8). This is expected as the moving wall effect is continuing to generate damping at the critical flow conditions (Fig. 3c).

F/A-18 Configuration

The analysis in Ref. 11 demonstrated that similarity relationships greatly simplify the rotary aerodynamics in the domain of vortex interaction for the F/A-18. In this domain, which is in the heart of the poststall maneuvering envelope, rotary testing is hardly necessary by virtue of the relationships between the lateral degrees of freedom, except insofar as it is necessary to define the rolling moment C_l. However, comprehensive rotary balance testing is very necessary in the domain of viscous fluid/motion coupling,[3,4] both at angles of attack where vortex breakdown occurs on the wing, $\alpha < 32.5$ deg, and beyond the angle of attack at which breakdown has reached the wing apex,[11] $\alpha > \alpha_{st} \approx 52.5$ deg. In the case of aircraft that do not have LEXs, such as the F-14, the situation is much more complex, as the viscous fluid/motion coupling dominates at $\alpha > 2\theta_A$ (Ref. 18). For the F/A-18 the onset of asymmetric vortex shedding in the static case occurs at $\alpha = \alpha_{on} \approx 57.5$ deg. At $\alpha > \alpha_{on}$ the baseline $C_n(\Omega)$ characteristics are similar to the body-alone characteristics at the same Reynolds number, with the same threshold $|\Omega_T| \approx 0.1$, which demonstrates that the yawing moment derives from the loading on the forebody.[11]

Vortex breakdown reaches the LEX apex at α near 47.5 deg, at symmetric conditions in laminar flow,[9] and at lower α at significant local sideslip angles. This is in agreement with the boundaries of vortex interaction correlation discussed in Ref. 11, and with recent flow visualization results.[19] Orbital platform coning rig (OPLEC) tests[10] showed that steady-state hysteresis occurs in the range $55 < \alpha < 67.5$ deg. At $\alpha = 60$ deg flow visualization demonstrates[19] that for high rates, for example, $\Omega = \pm 0.22$, vortex detachment flips to the advancing side whenever the rotation direction is reversed (Fig. 11), in agreement with Figs. 5b and 6. However, at low rates, $\Omega = \pm 0.10$, flowfield inertia effects dominate, and both flowfield asymmetries are possible (Fig. 12). The yawing moment $C_n(\Omega)$ at $\alpha = 60$ deg (Fig. 13), shows a highly definitive hysteresis loop. For motions initiated outside the loop the behavior is very steady (Fig. 11), but when the motion starts within the loop a high degree of unsteadiness exists, which signals the occurrence of apparently random bifurcations between the opposing conditions (Fig. 12). For instance, if at $\alpha = 65$ deg the motion is initiated at $\Omega_s = -0.2$, that is, $|\Omega_s| < \Omega_T$, $C_n(\Omega)$ will switch between the two branches for $-0.2 < \Omega < 0$ whenever the separation asymmetry is reversed (Fig. 14).

Note that the $C_n(\Omega)$ results are acquired from the DC-averaged measurements over a number (one or more) of complete coning revolutions and, therefore, do not contain any information on the dynamic overshoot associated with the change in rotation rate and/or direction. However, the unsteady behavior could be observed qualitatively through flow visualization.[19] From an examination of these results it is evident that, in the nonlinear domain at elevated angles of attack, alternatively deterministic or chaotic behavior will prevail, depending on whether or not the threshold rate Ω_T has been exceeded. While the two flow mechanisms, the coning-induced LEX bubble asymmetry, discussed earlier in connection with Fig. 5, and the moving wall effect[4] (Fig. 3), are in competition, the unsteady behavior will prevail. However, when Ω_T has been exceeded the moving wall effect is overpowered by the effect of nose microasymmetry, often amplified by support interference [except in the case of the OPLEC data,[9,10] (Figs. 14 and 15)], and the flow separation asymmetry becomes locked in, to remain in that flow state even if the threshold is subsequently crossed. This was confirmed in numerous flow visualization tests over several coning cycles.[19] There

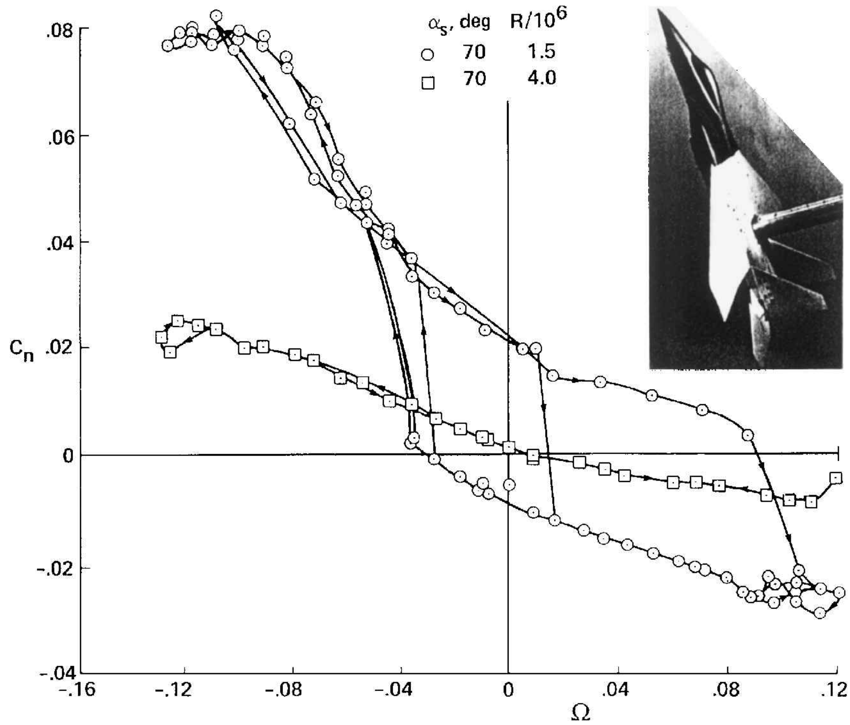

Fig. 9 Effect of support interference on F-15 aircraft model at α = 70 deg (Ref. 17).

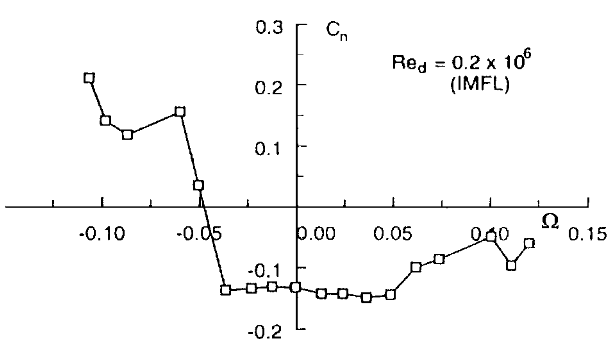

Fig. 10 Subcritical rotary data on WG16A aircraft model at α = 50 deg (Ref. 8).

is a great resistance to change from this flow state, and it will apparently prevail indefinitely in otherwise arbitrary maneuvers that do not cross the threshold.

As long as the aircraft motion does not exceed the threshold rate, in the range $|\Omega(t)| \leq \Omega_T$, the responses to arbitrary motions could not be satisfactorily represented by a convective time-lag model alone. Still, in principle, the rotary balance measurements represent the best source of data to investigate this phenomenon. The problem is that, to date, most rotary experiments in the nonlinear domain have apparently followed procedures that involve startup from $\Omega = 0$, thereby capturing the unsteadiness within the loop without defining the actual hysteretic behavior. One notable exception is the detailed rotary balance results on the F-15 (Fig. 9).[17] In the case of F/A-18, this loop is only partially captured in certain tests. Figure 15 shows that whereas the upper branch of the loop is captured in Ref. 20, subsequent NASA Langley Research Center tests (Bihrle Applied Research, Inc.) exhibited C_n on the two opposing branches at high rates, but with erratic behavior in between. The envelope of the data scatter coincides with the two branches at the higher rates. The data points midway between the two branches in the case of one of the NASA Langley Research Center data sets (Fig. 15) could indicate a neutral time average in the presence of frequent switching of the flow separation asymmetry. Recent water-tunnel flow visualization seems to indicate that an unsteady condition with apparent symmetric vortex shedding can result from the viscous fairing effect produced by dye injection.[19] However, this flow condition cannot be expected to materialize at turbulent flow conditions.

It can be argued that the damped characteristic is due to moving wall effects on transition at transitional Reynolds numbers.[12,14] Boundary-layer trips were not used in either the NASA Langley Research Center[20] or NASA Ames Research Center[21] tests. The latter data[21] were obtained at a near-critical Reynolds number, $Re = 0.16 \times 10^6$, which could explain the monotonic damping trend at $\alpha = 60$ deg (Fig. 15). The NASA Langley Research Center data[20] were clearly laminar at $Re_d = 0.05 \times 10^6$. For the F/A-18 there is some sensitivity to support interference[5] in both the vortex interaction and the viscous interaction regions.[11,19] In the former case, the principal effect of the support at low α is to deflect the attached forebody vortex, which prevents it from crossing over to interact on the advancing side,[19] thereby affecting the wing flowfields. In contrast, in the range $57.5 < \alpha < 67.5$ deg the attached forebody vortex dissipates above the canopy (i.e., well upstream of the support), whereas the lifted vortex misses the top-mounted support[11] (Fig. 16). Therefore, the main effect of support interference in this α range is its contribution to flow unsteadiness, rather than to flow nonuniformity. It was found that once the bifurcation threshold Ω_T had been exceeded, this threshold occurred at a lower rate in the presence of support interference (Fig. 17). When the threshold is not crossed, as in the case of Fig. 18, $|\Omega(t)| \leq 0.1$, large interference effects were observed.

Previous studies have found that sensitivity to support oscillation can be significant in the range of asymmetric vortex shedding.[22] It is likely that support oscillation played a role in producing the irregular data trend in Fig. 15. Support oscillations on the rotary rig in the NASA Langley Research Center spin tunnel[23] (Fig. 16) are perhaps an order of magnitude greater than in the OPLEC apparatus owing to the large difference in stiffness.[24] The resulting coupling with the moving wall effect, which is effective in the presence of unsteadiness,[4] is likely to have caused the erratic variations in the time-averaged measurements.

Interpretation of Incomplete Rotary Data

It seems likely in the light of recent results[10,19] on F/A-18 that, contrary to what the authors had surmised,[2] the threshold rate Ω_T had in fact not been determined on the AGARD WG16A model

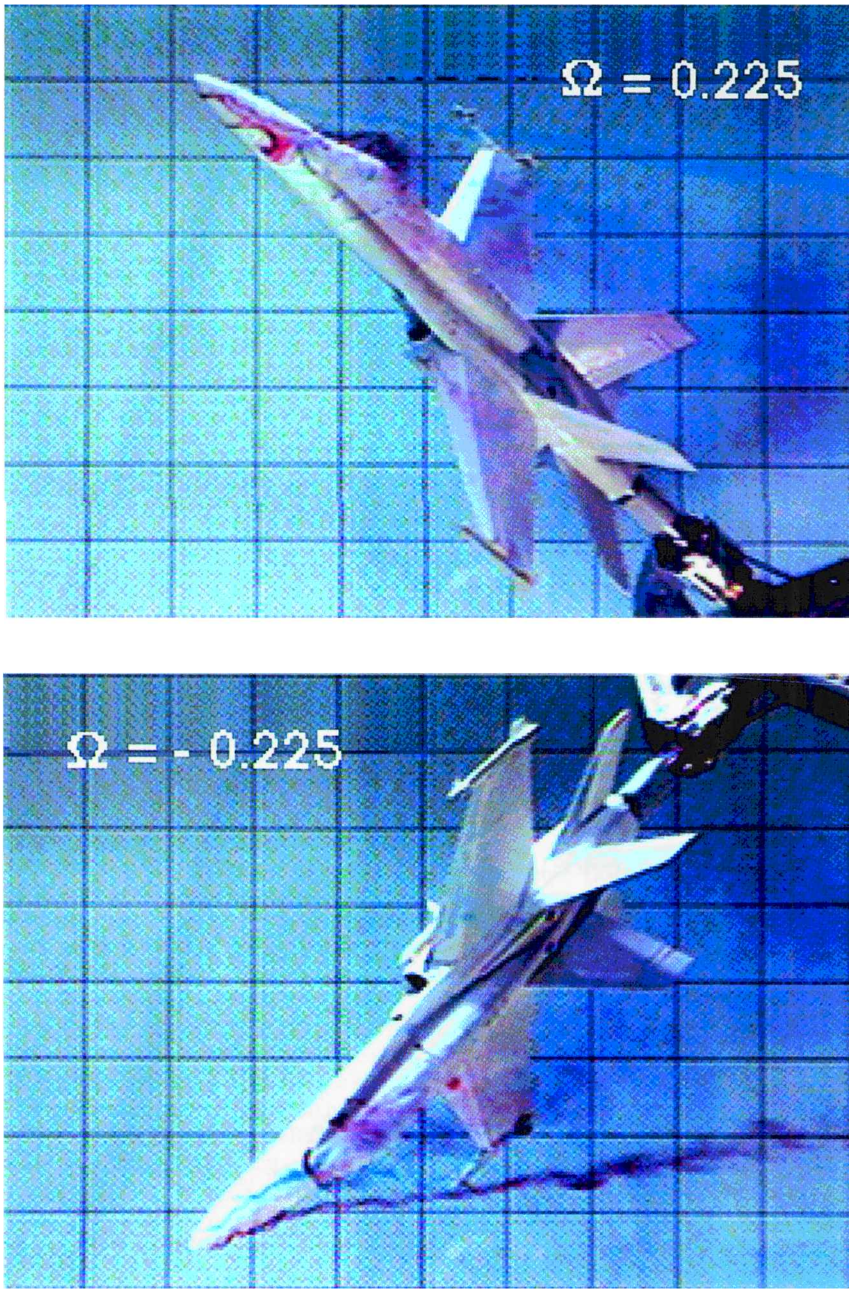

Fig. 11 Vortex flow on F/A-18 model coning at α = 60 deg and Ω = ± 0.225 (Ref. 19).

at $\alpha = 40$ deg and that most of the data points were in the range of flow unsteadiness. As the steady-state hysteresis had not been investigated in the AGARD experiment,[8] the deterministic aspect of the rotary characteristics had not been found. In the numerous tests made with boundary layer trips,[8] the result was only to complicate further the subscale rotary aerodynamics[12] to a point where interpretation was nearly impossible. However, at $\alpha = 50$ deg the $C_n(\Omega)$ characteristics were very steady at $|\Omega| < \Omega_T$ because of the dominant effect of the flow inertia. At $\alpha = 50$ deg $\gg 2\theta_A$ the moving wall effect is well outside its range of peak effectiveness, $\theta_A < \alpha < 2\theta_A$, whereas for the F/A-18 the hysteretic data were obtained at $\alpha \geq 57.5$ deg $\approx 2\theta_A$, where the moving wall effect is still able to compete with the kinematic coupling effect.

In attempting to utilize rotary data sets such as those in Figs. 8 and 10, the flight dynamicist has no choice but to speculate on the form of the missing data. Otherwise, the value of the data set would be very limited indeed. In the case of WG16A the test procedure was a simple speed-up of the rotation from the stationary condition, where the flowfield asymmetry could only be fixed in the quiescent position. If the rotation sequence could have been initiated at $\Omega < \Omega_T < 0$, the yawing moment response would have followed the upper branch. As in the case of F/A-18, if the sequence could have been initiated at a rate below the threshold, but with the flowfield asymmetry displaced to the opposite side, then the dominance of the support interference at low rates would have been broken and would have given way to considerable unsteadiness. Again, this illustrates how under different motion conditions the bistable aerodynamic characteristics can either be steady or degenerate into chaotic behavior.

The awkward reality for flight mechanics predictions and control system design is that much of the poststall maneuvering envelope may lie within the domain of unsteadiness, where the test results presented here have confirmed the chaotic nature of the vehicle aerodynamic responses. Moreover, much of the dynamic data generated to date in the nonlinear domain are restricted to this region and do not provide information on the basic hysteretic behavior. Inappropriate implementation in a six-degree-of-freedom (DOF) simulation can lead to misleading results. To avoid this, comprehensive investigation of steady-state hysteresis, support interference, and

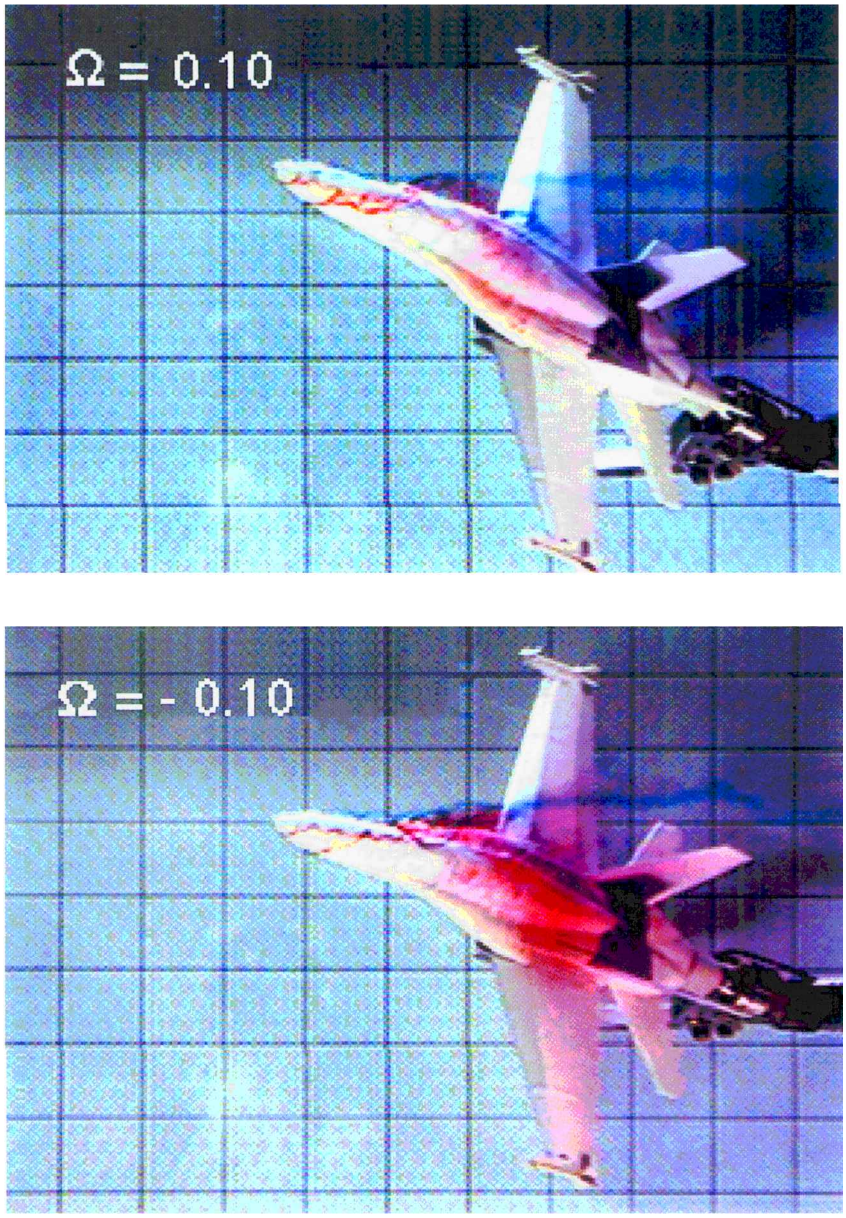

Fig. 12 Vortex flow on F/A-18 model coning at α = 60 deg and $\Omega = \pm\,0.10$ (Ref. 19).

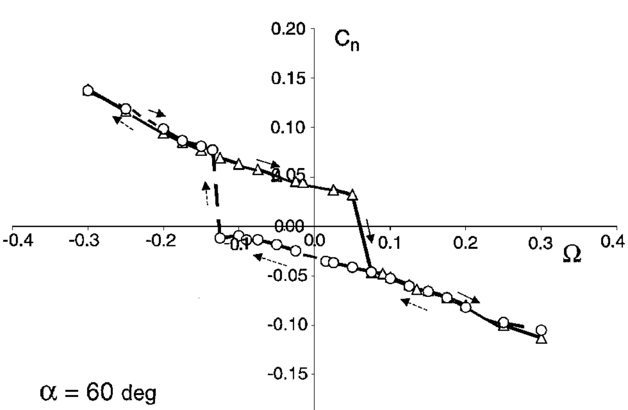

Fig. 13 OPLEC water-tunnel results for F/A-18 aircraft model at α = 60 deg, with rotation sequence initiated at $|\Omega_s| > \Omega_T$ and direction indicated by arrows.[10]

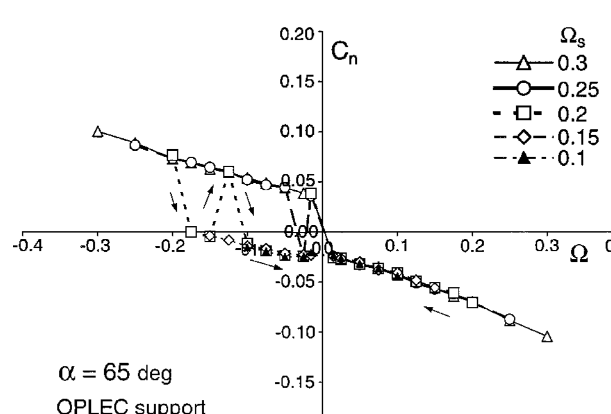

Fig. 14 OPLEC water-tunnel results for F/A-18 aircraft model at α = 65 deg, with rotation sequence initiated at $|\Omega_s| < \Omega_T$; direction of rotation sequence shown for Ω_s = 0.2 (Ref. 10).

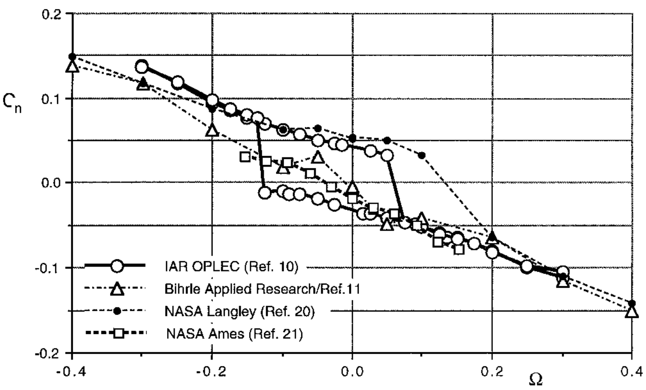

Fig. 15 Interfacility comparison of F/A-18 yawing moment at α = 60 deg.

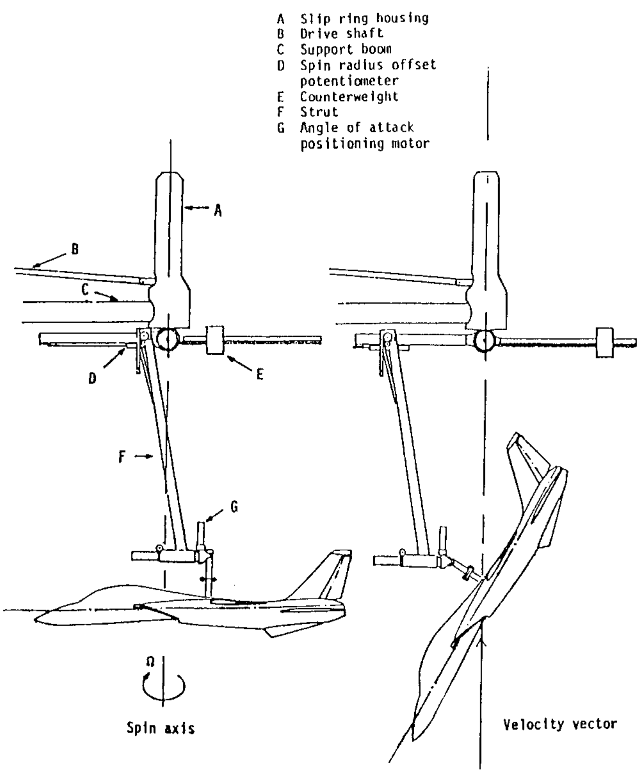

Fig. 16 Rotary balance apparatus in the NASA Langley Research Center Spin Tunnel.[23]

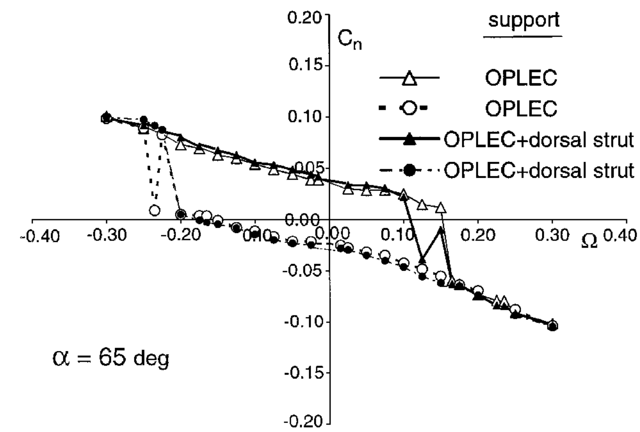

Fig. 17 Effect of dorsal strut in water-tunnel test of F/A-18 for $|\Omega_s| > \Omega_T$ (Ref. 10).

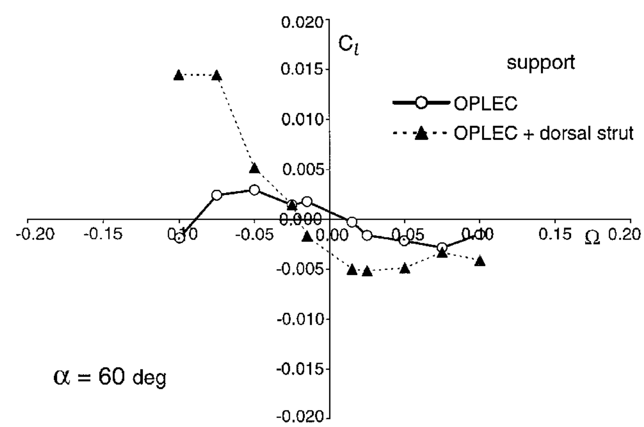

Fig. 18 Effect of dorsal strut in water-tunnel test of F/A-18 for $|\Omega_s| < \Omega_T$ (Ref. 10).

support oscillation is necessary. Because the WG16A results have shown the threshold rate to be insensitive to viscous flow effects for $0.2 \times 10^6 \leq Re \leq 0.3 \times 10^6$, the subcritical and supercritical behavior can be modeled[11] for rotation rates beyond the threshold. For the intermediate range bracketed by the threshold conditions, modeling of the viscous fluid/motion coupling and interference effects would be necessary. Because of the strong time-history dependence these coupling effects would have to be determined in two-DOF nonplanar dynamic tests.[11]

Because viscous and kinematic fluid/motion coupling characteristics are highly configuration dependent, it would not be wise to generalize. Nevertheless, in the case of LEX-dominated configurations a fairly clear picture has emerged. The relative degree of sensitivity to viscous fluid/motion coupling is strongly dependent on LEX/forebody shape and explains some of the differences between the behavior of the WG-16A model[2,12,25] and F/A-18 (Refs. 11 and 26).

The key focus in simulation of vehicle dynamics is on appropriate test conditions rather than on the volume of data that could be generated. Moreover, data quality could be considered satisfactory only if the flow physics relevant to free flight is captured.[2,7] Prior to definition of the test matrix, support and wall interference have to be investigated on the basis of previous experience[2,5–7,9,12] and/or exploratory tests. For practical reasons, the bulk of the database will be obtained at subcritical Reynolds numbers. Therefore, because it is imperative that the subcritical flow mechanisms be well understood, boundary-layer trips should not be used.[12] The steady-state hysteresis must be fully documented,[11] which will allow the motion parameter ranges to be deduced.

Conclusions

An analysis of nonlinear rotary balance data in the range of asymmetric vortex shedding, obtained on two aircraft configurations having prominent LEXs, has revealed the following:

1) A threshold coning rate exists that signals the onset of unsteadiness leading to bifurcation. Identification of this condition, including the definition of the steady-state hysteresis, is necessary for the implementation of the nonlinear rotary data.

2) Results on the generic aircraft model demonstrate that the threshold coning rate is determined by the motion-induced LEX upwash differential and the dynamic support interference.

3) The F/A-18 rotary data show evidence of time-history dependence, with alternately deterministic and chaotic responses resulting, depending on whether or not the threshold rate is exceeded.

4) In the nonchaotic flow regime the role of support interference is to increase the level of unsteadiness, thereby causing the threshold to shift to a lower coning rate.

5) Whereas modeling of the nonlinear responses should be tractable in the deterministic range, in the unsteady domain careful modeling of the viscous fluid/motion coupling would be required.

Acknowledgments

This research project was funded in part by the Department of National Defence, Canada. The authors appreciate the cooperation of the U.S. Navy in releasing the F/A-18 data set in Fig. 15, and the cooperation N. O'Connor of Bihrle Applied Research, Inc. for making the data available.

References

[1]Ericsson, L. E., and Reding, J. P., "Analytic Extrapolation to Full-Scale Aircraft Aerodynamics," *Journal of Aircraft*, Vol. 21, No. 3, 1984, pp. 222–224.

[2]Beyers, M. E., and Ericsson, L. E., "Extraction of Subscale Free-Flight Aerodynamics from Rotary Tests of Combat Aircraft," AIAA Paper 97-0730, Jan. 1997.

[3]Ericsson, L. E., and Beyers, M. E., "Viscous-Flow/Vehicle Motion Coupling," *Rotary Balance Testing for Aircraft Dynamics*, AR-265, AGARD, 1990, Chap. 8, pp. 164–167, 183–187.

[4]Ericsson, L. E., and Beyers, M. E., "Universality of the Moving Wall Effect," *Journal of Aircraft*, Vol. 37, No. 3, 2000; also AIAA Paper 99-0647, Jan. 1999.

[5]Ericsson, L. E., "Another Look at High-Alpha Support Interference in Rotary Tests," *Journal of Aircraft*, Vol. 28, No. 9, 1991, pp. 584–591.

[6]Beyers, M. E., and Ericsson, L. E., "Ground Facility Interference on Aircraft Configurations with Separated Flow," *Journal of Aircraft*, Vol. 30, No. 5, 1993, pp. 682–688.

[7]Beyers, M. E., "Interpretation of Experimental High-Alpha Aerodynamics Implications for Flight Prediction," *Journal of Aircraft*, Vol. 32, No. 2, 1995, pp. 247–261.

[8]AGARD Fluid Dynamics Panel Working Group 16, "Cooperative Programme on Dynamic Wind Tunnel Experiments for Manoeuvring Aircraft," edited by M. E. Beyers, AR-305, AGARD, Oct. 1996.

[9]Cai, H. J., and Beyers, M. E., "OPLEC Rotary Experiments on the F/A-18," National Research Council, LTR-A-021, Ottawa, ON, Canada, March 1998.

[10]Cai, H. J., and Beyers, M. E., "OPLEC Investigation of F/A-18 High-Alpha Aerodynamic Nonlinearities," National Research Council, LTR-A-046, Ottawa, ON, Canada, Dec. 1999.

[11]Beyers, M. E., "F/A-18 Nonplanar Manoeuvring Aerodynamics," *Proceedings of the 46th Annual Conference of Canadian Aeronautics and Space Institute*, (CASI), Ottawa, ON, Canada, May 1999, pp. 95–107.

[12]Ericsson, L. E., and Beyers, M. E., "Wind-Tunnel Aerodynamics in Rotary Tests of Combat Aircraft Models," *Journal of Aircraft*, Vol. 35, No. 4, 1998, pp. 521–528.

[13]Yoshinaga, T., Tate, A., and Inoue, K., "Coning Motion of Slender Bodies at High Angles of Attack in Low Speed Flow," AIAA Paper 81-1899, Aug. 1981.

[14]Ericsson, L. E., "Effects of Transition on Wind Tunnel Simulation of Vehicle Dynamics," *Progress in Aerospace Sciences*, Vol. 27, Pergamon, Oxford, England, UK, 1990, pp. 121–144.

[15]Bergmann, A., Hummel, D., and Oelker, H.-C., "Vortex Formation over a Close-Coupled Canard-Wing-Body Configuration in Unsymmetrical Flow," Paper 14, CP-494, AGARD, July 1991.

[16]Ericsson, L. E., and Reding, J. P., "Asymmetric Flow Separation and Vortex Shedding on Bodies of Revolution," edited by M. J. Hemsch, Vol. 141, Progress in Astronautics and Aeronautics, AIAA, Washington, DC, 1992, pp. 453–503.

[17]Malcolm, G. N., "Rotary Balance Experiments on a Modern Fighter Aircraft Configuration at High Reynolds Numbers," AIAA Paper 85-1829, Aug. 1985.

[18]Beyers, M. E., and Ericsson, L. E., "Unsteady Aerodynamics of Combat Aircraft Maneuvers," AIAA Paper 97-3647, Aug. 1997.

[19]Cai, H. J., and Beyers, M. E., "OPLEC Rotary Flow Visualization Study of F/A-18 at Zero Sideslip," National Research Council, LTR-A-042, Ottawa, ON, Canada, Aug. 1999.

[20]Hultberg, R., "Low Speed Rotary Aerodynamics of F18 Configuration for 0 to 90° Angle of Attack, Test Results and Analysis," NASA CR 3608, 1984.

[21]Kramer, B. R., Suarez, C. J., Malcolm, G. N., and Ayers, B. F., "F/A-18 Forebody Control, Volume 2, Rotary Balance Tests," NASA CR-45822, March 1994.

[22]Ericsson, L. E., "Lateral Oscillations of Sting-Mounted Models at High Alpha," *Journal of Aircraft*, Vol. 27, No. 5, 1990, pp. 508–513.

[23]AGARD Fluid Dynamics Panel Working Group 11, "Rotary Testing for Aircraft Dynamics," edited by M. E. Beyers, AR-265, AGARD, Dec. 1990.

[24]Beyers, M. E., and Huang, X. Z., "The Orbital Platform Concept for Nonplanar Dynamic Testing," National Research Council, NAE-AN-52, Ottawa, ON, Canada, May 1988.

[25]Ericsson, L. E., and Beyers, M. E., "Effect of LEX Surfaces on Lateral-Directional Dynamic Stability of Combat Aircraft," International Council of the Aeronautical Sciences, ICAS-98-1.4.2, Sept. 1998.

[26]Ericsson, L. E., and Beyers, M. E., "Why is LEX Vortex Breakdown on the F/A-18 Configuration Insensitive to Reynolds Number?," (submitted for presentation at AIAA Aerospace Sciences Meeting 2001).